Article

Metal-Free Oxidative Desulfurization Catalysts Based on Porous Aromatic Frameworks

Argam V. Akopyan, Leonid A. Kulikov, Polina D. Polikarpova,* Anna O. Shlenova, Alexander V. Anisimov, Anton L. Maximov, and Eduard A. Karakhanov
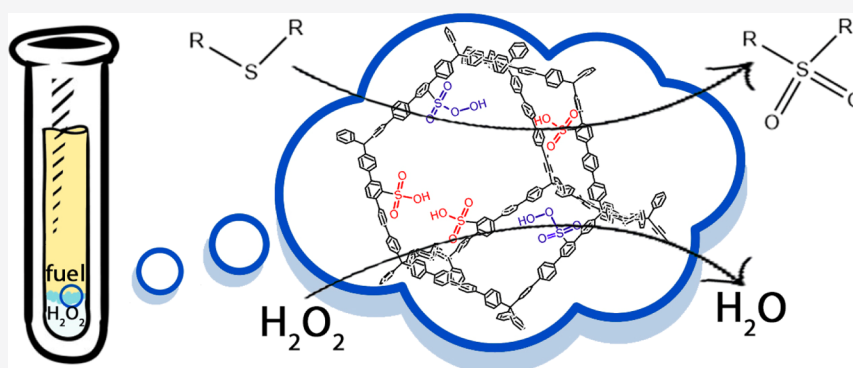
Read Online

ACCESS | Metrics & More | Article Recommendations

ABSTRACT: Porous aromatic frameworks modified by sulfonic groups were synthesized and, for the first time, applied for the oxidative desulfurization of a model and a real fuel. The main factors affecting the process including the catalyst dosage, temperature, reaction time, oxidant dosage, and hydrogen peroxide concentration were investigated in detail. Under optimal conditions, dibenzothiophene (DBT) was removed completely. It was shown that the synthesized catalysts reduced the sulfur content in the straight-run gasoline fraction up to ultra-low values (7 ppm). Fuel fractions and their oxidation products were analyzed by two-dimensional gas chromatography with time-of-flight mass spectrometry detection. No byproducts of hydrocarbon oxidation were found, which confirms the high selectivity of oxidation in the presence of synthesized catalysts. These catalysts retain their activity in DBT oxidation for at least five cycles.

1. INTRODUCTION

At present, much attention is being paid to environmental problems, particularly to air, soil, and water pollution caused by harmful emissions generated during cars' operation. Sulfur compounds are one of the dangerous components of fuels because they form sulfur oxide during combustion, are a source of acid rain, and cause harm to humans' health and other organisms.[1,2] Nevertheless, the demand for motor fuels is growing every year. In this regard, many countries have adopted EURO-5 requirements for motor fuels, limiting the sulfur content to values less than 10 ppm. The most common hydrotreatment method used to remove sulfur from petroleum distillates requires high capital and energy costs when implemented, which is not possible for small refineries. Therefore, it is necessary to develop alternative methods of desulfurization.[3,4]

Among the well-known non-hydrogen desulfurization methods, the most widespread method is oxidative desulfurization (ODS) which, in combination with the methods of adsorption and extraction, reduces the sulfur content in petroleum distillates by more than 99%.[5,6]

The ODS method includes two stages: the oxidation of sulfur-containing compounds and the extraction of oxidation products (sulfoxides and sulfones). Oxidation of sulfur-containing compounds occurs in the presence of an oxidant and a catalyst. The most common oxidizing agents are hydrogen peroxide because only water is formed as the byproduct.[7,8]

Currently, liquid-phase and heterogeneous catalysts are widely used in ODS.[2,9] A significant disadvantage of the former, limiting their widespread use, is its complexity and most often, the inability to regenerate. In this regard, researchers are

Table 1. Elemental Analysis and Amount of Chlorosulfonic Acid Used in PAF-30 Sulfonation

| material | amount of ClSO$_3$H, μL[a] | elemental analysis | | | | | the number of SO$_3$H groups, wt %[c] (content S, wt %) |
		C	H	S	O[b]	total	
PAF-30-SO$_3$H (1.0)	50	87.67	5.11	n.d.	n.d.	92.78	2.4 (0.94)
PAF-30-SO$_3$H (2.5)	100	78.88	4.68	2.41	3.62	89.59	5.9 (2.33)
PAF-30-SO$_3$H (5.0)	167	67.93	4.21	5.36	8.04	85.54	13.1 (5.18)
PAF-30-SO$_3$H (7.5)	250	58.26	4.19	8.53	12.80	83.78	21.1 (8.35)
PAF-30-SO$_3$H (10.0)	350	54.88	3.77	9.83	14.75	83.23	24.6 (9.70)
PAF-30-SO$_3$H (12.5)	500	52.13	3.34	11.28	16.92	83.67	27.8 (10.98)

[a]For sulfonation of 500 mg of PAF-30. [b]The oxygen content was calculated based on the amount of sulfur in the sample, assuming that sulfur and oxygen are present only as sulfo groups SO$_3$H. [c]The number of SO$_3$H groups determined by the acid−basic titration.

increasingly interested in heterogeneous catalysts containing transition metals that can form peroxocomplexes.[4,10,11]

Mesoporous materials are the most promising carriers for ODS catalysts due to the high surface area, optimal pore size for sulfur-containing compound diffusion, and a wide range of modification methods.[12−17] They differ in the structure of the pores, chemical composition, and the presence of "anchor" or ion-exchange groups, or Lewis or Bronsted acid centers. These properties of porous materials, in turn, determine the functional properties of the catalyst. One kind of mesoporous material, porous aromatic frameworks (PAFs), is of particular interest for the design of catalysts for ODS; their carbonic nature gives them a high affinity for organic compounds, including sulfur compounds, and due to the robust porous structure build of covalently linked aromatic building blocks, they possess high chemical and thermal stability. Recently, PAFs were used to create very active ODS catalysts based on molybdenum[18] and molybdenum-containing polyoxometalates.[13,19]

Salts or oxides of transition metals such as molybdenum, tungsten, and vanadium are most often used as the active phase because they can form a peroxocomplex in the presence of hydrogen peroxide.[10] However, there is a problem with leaching peroxocomplexes from the surface of the carrier. There are two ways to solve this problem: chemical immobilization of metals on the carrier or the use of metal-free catalysts. The choice of the first path leads to an increase in the number of catalyst synthesis stages and higher cost and does not always guarantee the absence of leaching of metals. Previously, we had shown that MCM-41-containing sulfonic groups can be used as a catalyst for the oxidation of the model compound dibenzothiophene (DBT).[20] However, the application of silica-based polar catalysts is connected with the fast catalyst deactivation due to the adsorption of polar oxidation products—sulfones in catalyst pores via hydrogen bond formation with silanol groups. To solve this problem and increase the surface's hydrophobicity, sulfonic groups containing PAFs were synthesized. It is important to note that the literature does not include data on using such materials in oxidation reactions.

2. EXPERIMENTAL SECTION

2.1. Chemicals. Trityl chloride (C$_6$H$_5$)$_3$CCl (purity, ≥97.0%, Sigma-Aldrich); aniline C$_6$H$_5$NH$_2$ (ReagentPlus grade, 99%, Sigma-Aldrich); hypophosphorous acid solution H$_3$PO$_2$ (50 wt % in water, Sigma-Aldrich); bromine Br$_2$ (reagent grade, Sigma-Aldrich); palladium(II)acetate Pd(OAc)$_2$ (reagent grade, 98% Sigma-Aldrich); triphenylphosphine PPh$_3$ (ReagentPlus, 99%, Sigma-Aldrich); 4,4′-biphenyldiboronic acid (HO)$_2$BC$_6$H$_4$C$_6$H$_4$B(OH)$_2$ (95.0%, ABCR Chemie Rus); dichloromethane (99%, Component-Reactive); tetrahydrofuran (THF) C$_4$H$_8$O (99%, Component-Reactive); chlorosulfonic

acid ClSO$_3$H (99%, Sigma-Aldrich); hydrogen peroxide H$_2$O$_2$ (50 wt, "Prime Chemicals Group"); dodecane n-C$_{12}$H$_{26}$ (99%, "Labteh"); DBT C$_{12}$H$_8$S (98%, Sigma-Aldrich); 4-methyldibenzothiophene (MeDBT) C$_{13}$H$_{10}$S (96%, Sigma-Aldrich); 4,6-dimethyldibenzothiophene (Me$_2$DBT) C$_{14}$H$_{12}$S (97%, Sigma-Aldrich); benzothiophene (BT) C$_8$H$_6$S (98%, Sigma-Aldrich); and 5-methylbenzothiophene (MeBT) C$_9$H$_8$S (98%, Sigma-Aldrich) were used as received.

Straight-run gasoline and diesel fractions with total sulfur contents of 700 and 2500 ppm, respectively, were used as industrial feedstock.

2.2. Synthesis. The PAF, PAF-30, was synthesized via the Suzuki cross-coupling reaction between tetrakis-(p-bromophenyl)methane and 4,4′-biphenyldiboronic acid according to the method described earlier.[18,21,22]

Sulfonation of PAF-30 was performed using a solution of chlorosulfonic acid in dichloromethane. PAF-30 (500 mg) was suspended in dichloromethane (25 mL), and the suspension was cooled to 0 °C. The required amount of chlorosulfonic acid (50−500 μL, see Table 1) was slowly added to the reaction medium. After adding all the chlorosulfonic acid, the mixture was stirred for a day at room temperature. After completion of the reaction, the suspension was poured into ice, the solid product was filtered, washed twice with water and twice with THF, and dried in a vacuum.

2.3. Characterization. All the materials were characterized by Fourier transform infrared (FTIR) spectroscopy, N$_2$ physical adsorption, and elemental analysis.

The number of sulfonic groups was determined by acid−base titration. 0.1 g of the catalyst was dissolved in 5 mL of NaOH (0,045 M) and stirred for 5 min. Then, 3−4 drops of the methyl orange indicator were added to a flask. The resulting mixture was titrated with HCl (0.025 M) solution until the solution's color changed from yellow to red. The experiment was performed at least three times with an error of less than 1%.

FTIR spectra were recorded using a Nicolet IR2000 (Thermo Scientific) spectrometer equipped with the multireflection horizontal attenuated total reflection accessory with a ZnSe crystal. Spectra were obtained using multiple distortions of the total internal reflection method in the range of 4000−500 cm^{-1} with a resolution of 4 cm^{-1}. All spectra were taken by averaging 100 scans.

The texture of the PAF-30 material was measured at the temperature of liquid nitrogen using a Gemini VII 2390 V1.02t (Micrometics) automated surface area analyzer. Before the analysis, the sample was degassed at 120 °C and 0.01 mbar overnight. The analysis range of relative pressure was 0.05−0.99 p/p_0. The specific surface area (S_{BET}) was calculated using the Brunauer−Emmett−Teller (BET) model. The total pore volume was measured at a p/p_0 value of 0.99. The pore volume

was determined using the Barrett−Joyner−Halenda model. The pore size distribution was calculated using SAIEUS Program, version 3.0 (Demo), and NLDFT model with a kernel for carbon materials with slit pores.

Chemical composition was determined in a Thermo Flash 2000 elemental analyzer in the Center for Collective Usage "Analytical Center for the Problems of Deep Refining of Oil and Petrochemistry" of A.V.Topchiev Institute of Petrochemical Synthesis, RAS.

2.4. Oxidation of a Model Fuel. The model fuel of sulfur-containing compounds [DBT (Sigma-Aldrich), BT (Sigma-Aldrich), MeBT (Sigma-Aldrich), MeDBT (Sigma-Aldrich), and Me$_2$DBT (Sigma-Aldrich)] used to study the activity of catalysts contained 500 ppm of sulfur. The fuel volume in each reaction was 5 mL, and dodecane (C$_{12}$H$_{26}$, Sigma-Aldrich) was used as the solvent. Oxidation was carried out according to the following method: the model fuel was heated to the reaction temperature, then 0.0025−0.0180 g of the catalyst and 7−40 μL of the 50% hydrogen peroxide solution (based on the ratio [O]/S = 2:1−12:1) were added with stirring. The mixing speed in all the experiments was the same and was 650 rpm.

After the reaction was completed, the fuel was separated from the catalyst and oxidant and analyzed by gas chromatography (GC) using a Crystal-2000M set [flame ionization detector; column, Zebron; L, 30 m; d, 0.32 mm; liquid phase, ZB-1] while programing the temperature from 100 to 250 °C (the carrier gas is helium). Chromatograms were recorded and analyzed using the ChromaTech Analytic 1.5 program.

Figures 4−10 show the average values of the three converging results. The experimental error is no more than 5%.

2.5. Desulfurization of the Real Fuel. According to the following procedure, desulfurization of the real fuel was carried out as follows: 0.018 g of the catalyst and 0.04 mL of hydrogen peroxide were added to 10 mL of the fuel. The oxidation reaction was carried out for 60 min at 70 °C. After oxidation, the reaction mixture was passed through 1 g of silica gel to remove the oxidized products.

The total sulfur content in hydrocarbon fractions was determined using a sulfur analyzer ASE-2 (energy-dispersive analyzer of sulfur) according to the ASTM D 4294-10 standard. The method is based on X-ray fluorescence energy-dispersive spectrometry, allowing the determination of the sulfur mass fraction in the diesel fuel and unleaded gasoline in the range of 7−50000 ppm with a relative error of 3%.

Each experiment was made repeatedly to obtain a minimum of three convergent results (the concurrent result is a result that differs from the average value of no more than 5%). An average of the performed experiments is reported in the article. The measurement error is not more than 5%.

2.6. 2-D GC with Time-of-Flight Mass Spectrometry and Flame Ionization Detection. Analysis of gasoline and diesel fractions was conducted by two-dimensional GC with time-of-flight mass spectrometry and flame ionization detection (GC × GC−TOFMS−FID) on a Leco Pegasus GC-HRT 4D. The instrument includes an Agilent 7890A gas chromatograph with an embedded second oven, a flow splitter, a flame ionization detector, a two-stage cryomodulator, and a Leco Pegasus 4D time-of-flight mass analyzer. Analysis conditions are given below:

- Injector: temperature, 300 °C; sample volume, 0.2 μL; carrier gas, helium; flow rate through the column, 1 mL/min; split ratio, 500; injector (septum) purge flow rate, 3

mL/min; and operating mode, pressure adjusted to maintain a constant flow rate.

- Chromatographic separation: column 1, polar; phase, Rxi-17Sil (30 m × 0.25 mm × 0.25 μm); column 2, nonpolar; and phase, Rxi-5Sil (1.7 m × 0.10 mm × 0.10 μm). Temperature regime of the first oven: initial temperature, 40 °C (2 min); heating to 320 °C at a rate of 3 °C/min; and holding for 5 min. The second oven temperature and the modulator are maintained at levels of 6 and 21 °C higher than the temperature of the first oven, respectively. Modulation time on the modulator is 6 s.

- Flame ionization detector: temperature, 340 °C; H$_2$ flow rate, 40 mL/min; air flow rate, 450 mL/min; and blowing-in flow rate, 30 mL/min. The line to the detector is 1.4 m × 0.25 mm; the first oven sets the temperature.

- Mass detector: ion source temperature, 280 °C; frequency, 100 Hz; detected mass range, 35−520; recording rate, 100 spectra per second; and electron energy, 70 eV. The line to the detector is 3.0 m × 0.18 mm and temperature, 280 °C.

Analysis results were processed using CromaTOF software (Leco).

3. RESULTS

3.1. Catalyst Characterization. The reaction of the polymer provided the modification of PAF-30 with sulfo groups with chlorosulfonic acid (Figure 1). Low temperatures of
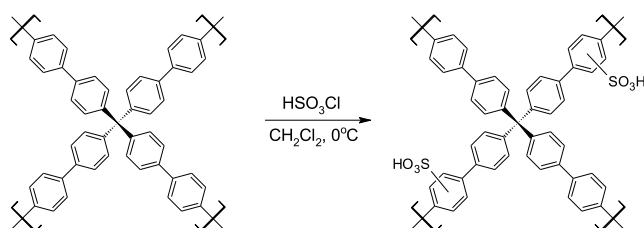

Figure 1. Sulfonation of PAF-30.

synthesis are necessary to minimize the possible degradation of the porous structure during the sulfonation. Thus, a series of materials were obtained with a nominal sulfur content from 1 to 12.5% (Table 1). In all cases, the total content of elements in the material is less than 100%, which is associated with the incomplete combustion of the material during analysis.[23,24]

The number of deposited sulfo groups was determined by the acid−base titration method (Table 1). The sulfur content in the synthesized catalysts was determined based on the number of sulfo-groups obtained by titration. According to the data obtained, the amount of sulfur determined by the elemental analysis method is consistent with the titration data. Thus, we have obtained a series of catalysts containing 2.4−27.8% of the SO$_3$H groups.

The sulfonation of PAF-30 resulted in a change in its color from colorless to blue-violet (Figure 2), and the intensity of the resulted color depends on the content of sulfo groups in it. This effect could be attributed to a charge transfer between the sulfo groups and benzene rings near them, and it is possible only in dry solids.[25] Thus, after placing any of the sulfonated polymers in water, its color becomes light yellow; after drying the resulting "wet" material in a vacuum, it regains its dark blue color. We should note that such a change in the color of the material to dark blue is characteristic not only for sulfonated PAFs but also

Figure 2. Sulfonated polymers based on PAF-30 (from left to right): PAF-30-SO$_3$H (1) (yellow); PAF-30-SO$_3$H (2.5) (light-green); PAF-30-SO$_3$H (5) (green); PAF-30-SO$_3$H (7.5) (dark-green); PAF-30-SO$_3$H (10) (blue); and PAF-30-SO$_3$H (12.5) (dark blue).

in Lewis acid/PAF composites, such as AlCl$_3$/PAF-20 or FeCl$_3$/PAF-20,[26,27] and even when PAFs are placed in a strong acid solution (HF, HCl, HBr, etc.).

The confirmation of the introduction of −SO$_3$H groups in the structure of PAFs has been confirmed by FTIR spectroscopy (Figure 3); new absorbance bands appeared at 1370, 1135−1221, 1034, 901, and 610 cm^{-1}, and their intensity increases with the content of sulfo groups in the materials. The same IR spectrum pattern of sulfonated PAFs was observed in some previous studies.[23,28−30] Also, some signals of the initial framework were shifted. For instance, an absorbance band at 1485 cm^{-1} was shifted to 1464 cm^{-1}, 1117 to 1099 cm^{-1}, 808 to 823 cm^{-1}, and so forth. Such a shift could be the evidence of chemical modification of the polymer structure, confirming the introduction of sulfonic groups in the PAF, not simple absorbance of acid by the porous material. A similar shift was observed in ref 28 for PPN-6 and its sulfonated analogue PPN-6-SO$_3$H and in studies.[29,31,32]

The N$_2$ adsorption isotherm of PAF-30 is typical for materials with hierarchical micro- and mesoporous structures; there is a steep increase of the adsorption curve at low p/p_0 values and hysteresis between adsorption and desorption branches. The modification of PAF-30 with sulfo groups leads to the expected decrease in its surface area and pore volume (Table 2). Pore size distribution graphs for the obtained materials, based on the NLDFT model with a kernel for carbon materials with slit pores, show maxima in the micropore area (0.8−1.5 nm), "small" mesopore area (2.6−3.2 nm), and "large" mesopore area (20−30 nm). The latter type of pore can be attributed to the space

Table 2. Textural Characteristics of Synthesized Samples

material	SBET, m^2/g[a]	pore volume, cm^3/g	pore sizes, nm[b]
PAF-30	514	0.345	0.81; 2.7
PAF-30-SO$_3$H (1)	507	0.343	0.93; 2.7; 22
PAF-30-SO$_3$H (2.5)	455	0.365	0.97; 2.75; 22
PAF-30-SO$_3$H (5)	180	0.220	1.32; 2.8; 22
PAF-30-SO$_3$H (7.5)	145	0.155	1.48; 3.1; 22
PAF-30-SO$_3$H (10)	85	0.121	1.5; 2.7; 5; 21
PAF-30-SO$_3$H (12.5)	89	0.117	1.5; 2.6; 3.9; 22

[a]S$_{BET}$—surface area by the BET model. [b]maxima on the PSD graph.

between material particles, and the first two characterize the pores inside the PAF particles.

3.2. Oxidation of Model Fuels. The activity of synthesized catalysts was first studied on model fuels. The primary data are given for DBT's model fuel because it is one of the most difficult-to-remove diesel fraction components. Most researchers in ODS use this compound to study the effectiveness of catalysts in the oxidation of sulfur compounds. At the first stage, the dependence of DBT conversion on the number of sulfonic groups in the catalyst was studied (Figure 4). DBT was oxidized with a 50% solution of hydrogen peroxide as an oxidant.
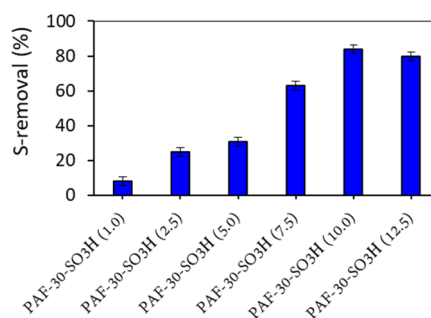
Figure 4. Effect of quantity of sulfonic groups on the conversion of DBT. Oxidation conditions: H$_2$O$_2$/S = 6:1 (molar), 9 mg of catalyst/5 mL of the model fuel, 70 °C, and 60 min.

Sulfonic groups immobilized to PAF-30 act as a source of active oxygen because persulfonic acid is formed in the presence of hydrogen peroxide. As the results of the experiment showed, increasing the number of sulfonic groups to 10% by weight
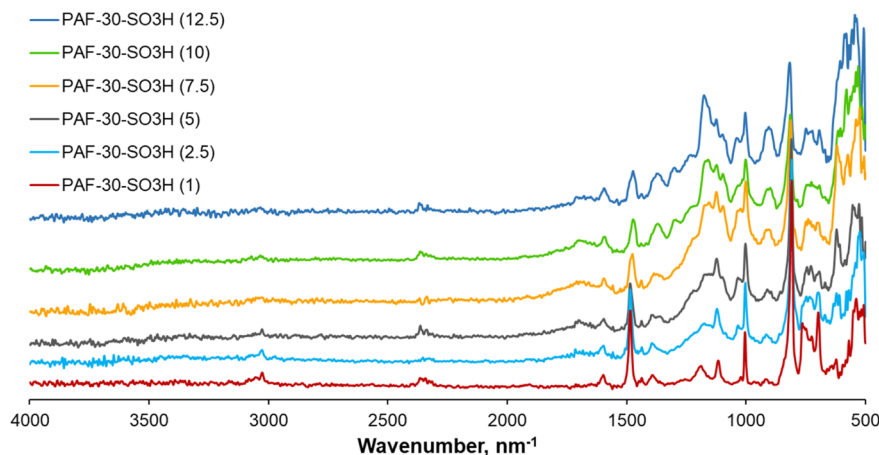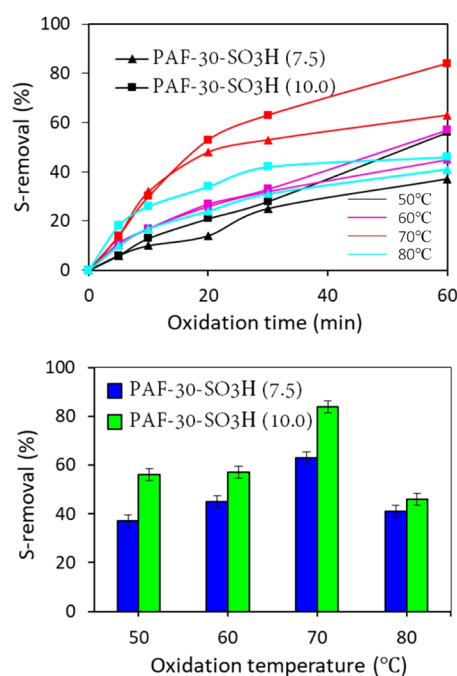

Figure 3. FTIR spectra of sulfonated materials.

improves the conversion of DBT; further increase of sulfonic group content to 12.5% leads to a slight decrease of DBT conversion which can, probably, be connected with a simultaneous pore volume decrease for PAF-30-SO₃H (Figure 4). A reduction in the pore size of the catalyst when a large number of substituents are applied can lead to steric difficulties. Thus, two catalysts with weight contents of sulfonic groups by 7.5 and 10% were chosen for further investigation.

The effect of temperature on DBT conversion was studied for two catalysts, PAF-30-SO₃H (7.5) and PAF-30-SO₃H (10.0). To study the DBT conversion, a temperature range from 50 to 80 °C with a step of 10 °C was selected.
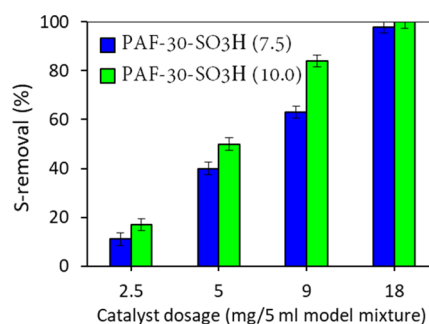
According to the data obtained (Figure 5) at 50 and 60 °C, it is possible to achieve more than 50% conversion, while

Figure 6. Effect of the catalyst dosage on the conversion of DBT. Oxidation conditions: H_2O_2/S = 6:1 (molar), 70 °C, and 60 min.

At a catalyst dosage of 9 mg/5 mL of the model fuel, the effect of the amount of the oxidant on the conversion of DBT was studied. The molar ratio of hydrogen peroxide to sulfur varied from 2:1 to 12:1. For the complete oxidation of DBT, a theoretically twofold excess of hydrogen peroxide is required; but during the oxidation reaction, the oxidizer is gradually diluted with water, which is formed as a result of the reaction which leads to a decrease in the rate of formation of persulfonic acid. Based on the data obtained (Figure 7), an increase in the

Figure 5. Effect of temperature on the conversion of DBT. Oxidation conditions: H_2O_2/S = 6:1 (molar), 9 mg of catalyst/5 mL of the model fuel, and 60 min (for the bottom figure).

Figure 7. Effect of the quantity of hydrogen peroxide on the conversion of DBT. Oxidation conditions: H_2O_2/S = 6:1 (molar), 9 mg of catalyst/ 5 mL of the model fuel, 70 °C, and 60 min.
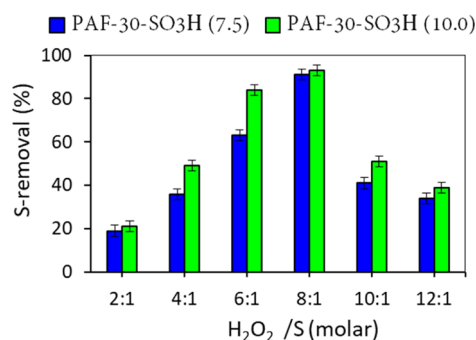
increasing the temperature to 70 °C leads to a significant improvement in the conversion rate associated with an increased rate of the formation of persulfonic acid. Raising the temperature to 80 °C reduces the conversion rate. This effect is related to an increase in the decomposition rate of hydrogen peroxide with increasing temperature, which leads to a decrease in the amount of persulfonic acid. In previous work,[20] for a MCM-based catalyst, the same results were obtained at a higher temperature of 80 °C. This fact can be connected with the adsorption of oxidation products—corresponding sulfone—on supports via hydrogen bonds with hydroxyl groups of mesoporous silicate MCM-41. In this regard, using a nonpolar polyaromatic framework as the catalyst support seems to be more preferable due to better results obtained at lower temperatures.

Changing the catalyst's dosage showed that 18 mg of the catalyst PAF-30-SO₃H (10.0) is enough to completely oxidize 500 ppm of the DBT (Figure 6). However, a decrease in the amount of the catalyst in the reaction leads to a reduction in the DBT conversion because of the low quantity of active catalyst sites.

amount of hydrogen peroxide from a twofold to a eightfold excess has a positive effect on the conversion of DBT. An increase in the amount of hydrogen peroxide in the reaction mixture leads to an increase in the amount of persulfonic acid, which reacts with DBT. The rise of oxidant amount can also result in a more quick reaction equilibrium. At the same time, as can be seen from Figure 7, a further increase above hydrogen peroxide to 10 and 12 leads to a sharp decrease in DBT conversion. This trend may be caused by filling the catalyst's pores with water present in the oxidant via hydrogen bond formation of water with sulfonic groups, thus preventing nonpolar substrate's adsorption on active sites.

The effect of hydrogen peroxide concentration on DBT conversion was also studied (Figure 8). This study was carried out while maintaining the molar ratio of H_2O_2/S = 6:1 in all the experiments. Thus, with a decrease in the hydrogen peroxide concentration, the amount of water in the system increased. The effect of the hydrogen peroxide concentration on the DBT conversion was performed in the presence of the catalyst PAF-30-SO₃H (10.0) that was most active in the oxidation reactions. The concentration of hydrogen peroxide varied from 10 to 50 wt %. Based on the data obtained (Figure 8), it can be concluded that a decrease in the concentration of hydrogen peroxide and,
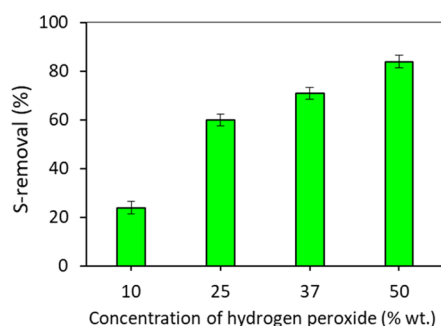
Figure 8. Effect of concentration of hydrogen peroxide on the conversion of DBT. Oxidation conditions: 9 mg of PAF-30-SO$_3$H (10.0)/5 mL of model fuel, 70 °C, and 60 min.

Figure 10. Recycling of the catalyst. Oxidation conditions: H$_2$O$_2$/S = 6:1 (molar), 9 mg of PAF-30-SO$_3$H (10.0)/5 mL of model fuel, 70 °C, and 60 min.

consequently, an increase in the amount of water in the reaction system leads to a significant decrease in the DBT conversion. Therefore, water, which is present as an integral component in the hydrogen peroxide solution, is partially adsorbed in the catalyst's pores, which prevents the substrate from approaching the catalyst's active centers. In this regard, to minimize the influence of water on the oxidation process, further research was carried out in the presence of 50 wt % hydrogen peroxide.

Because sulfur compounds of various classes are present in real petroleum products, it was essential to evaluate the possibility of using these catalysts to oxidate the sulfur-containing compounds of various structures. PAF-30-SO$_3$H (10.0) was selected as the most active catalyst. Oxidation was performed at 70 °C for 60 min. According to the data obtained (Figure 9), methyl substituents' presence leads to a decrease in
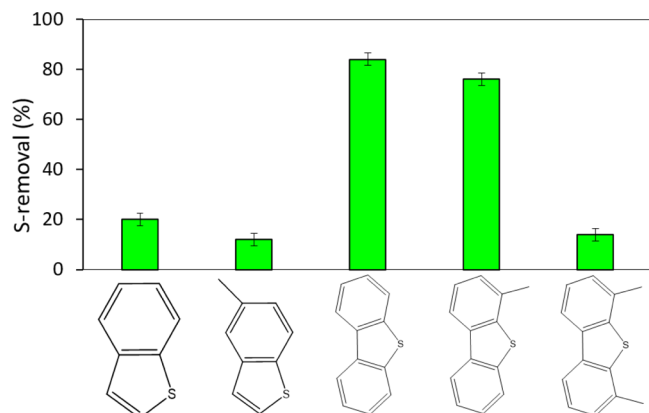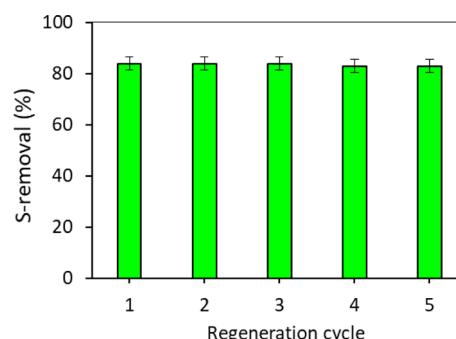

Figure 9. Oxidation of various classes of sulfur-containing compounds. Oxidation conditions: H$_2$O$_2$/S = 6:1 (molar), 9 mg of PAF-30-SO$_3$H (10.0)/5 mL of model fuel, 70 °C, and 60 min.

the conversion of sulfur compounds, associated with steric difficulties. Conversion of BT and its methyl derivative is much lower than the conversion of DBT, which is connected with a lower electron density on a sulfur atom in the BT molecule.[2]

An important characteristic of heterogeneous catalysts is the possibility of their regeneration. The regeneration of the catalyst was performed by washing with acetone, followed by drying the catalysts in a vacuum at 80 °C. After drying, the catalyst was reused.

As can be seen from Figure 10, the catalyst PAF-30-SO$_3$H can be reused for at least five cycles.

3.3. Kinetics of DBT Oxidation. According to the literature data,[33] the reaction of DBT oxidation to sulfones proceeds in the

pseudo-first-order. A linear section of the kinetic curve was selected for the calculation of the rate constant for 50, 60, and 70 °C for two different catalysts, PAF-30-SO$_3$H (7.5) and PAF-30-SO$_3$H (10.0). The reaction order has been checked by the graphical method using linearized coordinates "ln$(C_0/C_t) - t$", where C_0 is the initial concentration of DBT and C_t is the current one. Figure 11 has a linear form that corresponds to the correct choice of the reaction order.
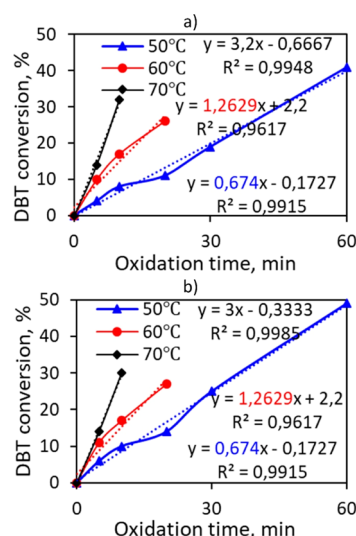
Figure 11. Initial sections of the DBT conversion dependence on the reaction time for (a) PAF-30-SO$_3$H (7.5) and (b) PAF-30-SO$_3$H (10.0).

For the first reaction order, the kinetic equations are:

$$-\frac{dc}{c} = k \, dt$$

$$\ln \frac{c_0}{c_t} = kt$$

The experimental data were plotted in the coordinates $\ln(C_0/C_t) - t$ (time, min^{-1}). The constants were calculated as the tangent of the slope of the curve for each catalyst. The data are shown in the Table 3.

3.4. Oxidative Desulfurization of Real Fuels. Because the obtained catalysts showed promising activity in the oxidation reactions of the model fuel, their activity in the ODS of the real fuel was studied. Straight-run gasoline with 700 ppm and diesel

Table 3. Calculated Rate Constants of the DBT Oxidation Reaction

catalyst	temperature and the constant		
	50 °C	60 °C	70 °C
PAF-30-SO$_3$H (7.5)	0.674	1.419	3.147
PAF-30-SO$_3$H (10.0)	0.793	1.469	2.951

fraction with 2500 ppm of the initial sulfur content was selected as a research object. Because real fuels contained more than 500 ppm, the oxidation of model DBT mixtures containing 1000 and 2000 ppm was carried out under the following conditions: H$_2$O$_2$/S = 6:1 (molar), 18 mg of PAF-30-SO$_3$H (10.0)/10 mL of the fuel, 70 °C, and 60 min. According to the data obtained, the DBT conversions were 95 and 83% in model mixtures of 1000 and 2000 ppm, respectively. The decrease in the activity of catalysts during the transition to model fuels with a high sulfur content is probably due to the adsorption of oxidation products in the catalyst pores. The oxidation of straight-run gasoline and diesel fractions was carried out under similar conditions.

ODS of straight-run gasoline and diesel fractions was performed in two stages. At the first stage, the oil fraction was oxidized. In the second stage, the oxidized sulfur compounds were extracted by adsorption on silica gel. As a result of desulfurization, it was possible to reduce the gasoline and diesel fraction's sulfur content by 99% (up to 7 ppm) and 71% (up to 725 ppm), respectively.

To assess which of the classes of sulfur compounds were removed during ODS, fuel fractions and their oxidation products were analyzed by two-dimensional gas chromatography with TOFMS detection. Previously, we successfully applied this method to analyze hydroprocessing products of the diesel fraction.[34,35] The chromatograms' general appearance suggests that the composition of both gasoline and diesel fractions is generally preserved (Figure 12). No byproducts of hydrocarbon oxidation—alcohols, phenols, carbonyl, and carboxyl compounds, were found, which confirms the high selectivity of oxidation in the presence of synthesized catalysts.

An analysis of all ions registered during the analysis was carried out to determine the composition of sulfur compounds in fuel fractions. All the ions of the composition C$_x$H$_y$S$_z$ were classified by the number of carbon atoms and the degree of unsaturation (ring and double bond equivalent, RDBE). It can be seen that sulfur compounds in gasoline (Figure 13) are represented by various mercaptans and sulfides (RDBE = 0–0.5), thiophanes (RDBE = 1–1.5), several polycyclic naphthenic sulfides (RDBE = 2–4), and benzothiophene (RDBE = 6–6.5) and some DBT (RDBE = 9–9.5) derivatives. It can be noted that during the treatment, most of the easily oxidized compounds are removed and after oxidation in gasoline, sulfur compounds are mainly represented by benzothiophenes and DBTs (Figure 14).

In the case of diesel fuel, the reduction of sulfur compounds also occurs mainly due to the removal of easily oxidizable sulfur compounds (RDBE < 6) (Figure 15). Ions from benzo- and DBTs retain their intensity, which indicates a low rate of their oxidation. The results obtained correlate with the rate of oxidation of model compounds (Figure 9). Thus, the obtained
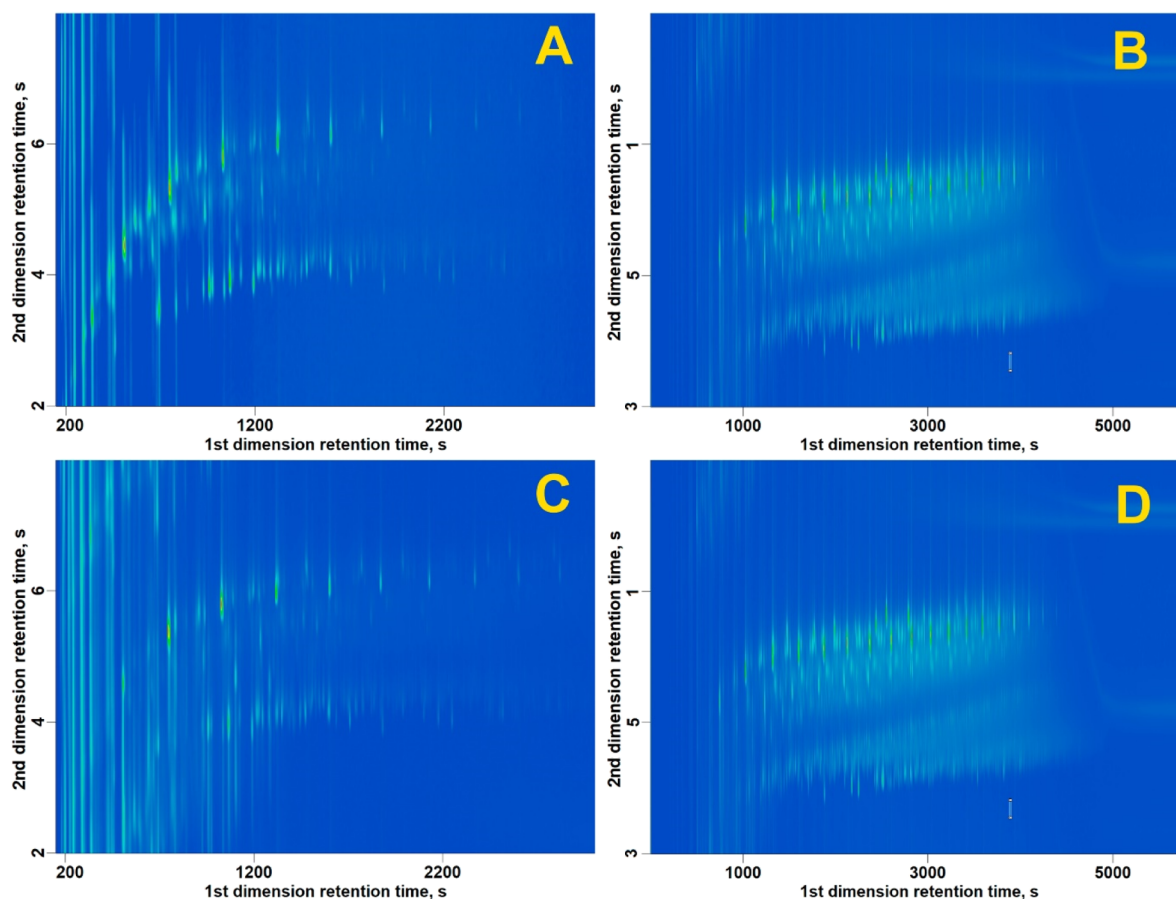
Figure 12. 2D-chromatograms of raw gasoline (A) and diesel (B) and products after desulfurization (C and D, respectively).
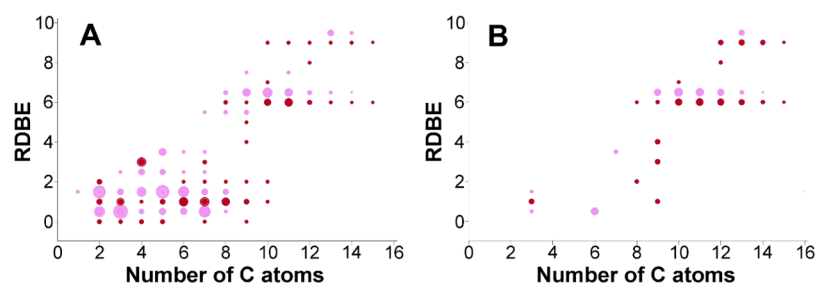
Figure 13. Ring and double-bond equivalent versus carbon number plots for ions in raw gasoline (A) and gasoline after oxidative treatment (B).
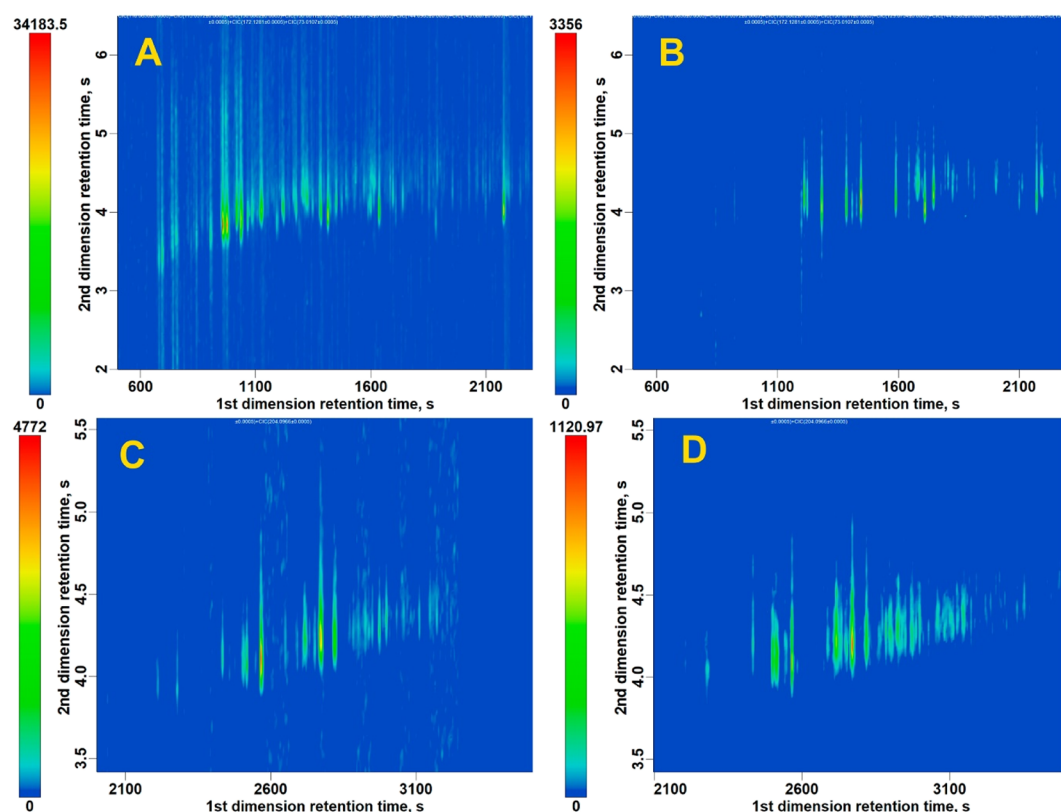

Figure 14. Signals from thiophanes (ions with RDBE = 1−1.5) and benzothiophenes (ions with RDBE = 6−6.5) in raw gasoline (A and C, respectively,) and gasoline after treatment (B and D, respectively).
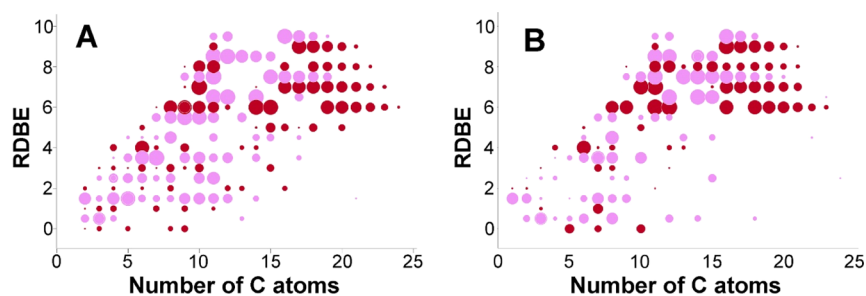

Figure 15. Ring and double-bond equivalent versus carbon number plots for ions in raw diesel (A) and diesel after oxidative treatment (B).

catalysts can be used for the desulfurization of real fuel fractions; however, removing sterically hindered substrates is still a problem to be solved.

4. CONCLUSIONS

The possibility of using sulfated PAFs as catalysts for ODS was shown for the first time. This catalyst proved to be useful for ODS both for model and real fuels. The synthesized catalytic systems have potential due to the high activity in oxidative reaction media, easy separation from reaction products, and high affinity toward aromatic substances through the formation of $\pi-\pi$ interactions. The main factors affecting the conversion of DBT are as follows: catalyst dosage, sulfonic group content, reaction temperature, and hydrogen peroxide concentration.

DBT was oxidized completely in optimal conditions, and sulfur content in the straight-run gasoline fraction was reduced up to ultra-low values (7 ppm). Two-dimensional gas chromatography analysis with TOFMS detection shows no oxidation byproducts of hydrocarbon oxidation, which confirms the high selectivity of oxidation in the presence of synthesized catalysts. The immobilization of catalyst's active sites on the surface via the covalent bond allows preventing leaching of sulfonic groups. Thus, synthesized catalysts retain activity in DBT oxidation for at least five cycles of oxidation regeneration..

■ AUTHOR INFORMATION

Corresponding Author

Polina D. Polikarpova − *Chemistry Department, Lomonosov Moscow State University, 119991 Moscow, Russia;* ⊙ orcid.org/0000-0002-0456-8248; Email: polikarpova@petrol.chem.msu.ru

Authors

Argam V. Akopyan − *Chemistry Department, Lomonosov Moscow State University, 119991 Moscow, Russia;* ⊙ orcid.org/0000-0001-6386-0006

Leonid A. Kulikov − *Chemistry Department, Lomonosov Moscow State University, 119991 Moscow, Russia;* ⊙ orcid.org/0000-0002-7665-5404

Anna O. Shlenova − *Chemistry Department, Lomonosov Moscow State University, 119991 Moscow, Russia;* ⊙ orcid.org/0000-0003-3907-3701

Alexander V. Anisimov − *Chemistry Department, Lomonosov Moscow State University, 119991 Moscow, Russia;* ⊙ orcid.org/0000-0001-9272-2913

Anton L. Maximov − *Chemistry Department, Lomonosov Moscow State University, 119991 Moscow, Russia; A.V.Topchiev Institute of Petrochemical Synthesis, 119991 Moscow, Russia*

Eduard A. Karakhanov − *Chemistry Department, Lomonosov Moscow State University, 119991 Moscow, Russia;* ⊙ orcid.org/0000-0003-4727-954X

Complete contact information is available at:
https://pubs.acs.org/10.1021/acs.iecr.1c00886

Author Contributions

All the authors contributed equally. The manuscript was written through the contributions of all the authors. All the authors have approved the final version of the manuscript.

Notes

The authors declare no competing financial interest.

■ ACKNOWLEDGMENTS

■ ABBREVIATIONS

ODS   oxidative desulfurization methods
PAFs   porous aromatic frameworks
FTIR   Fourier transform infrared
BET   Brunauer−Emmett−Teller
BJH   Barrett−Joyner−Halenda
DBT   dibenzothiophene
BT   benzothiophene
MeBT   5-methylbenzothiophene
MeDBT   4-methyldibenzothiophene

■ REFERENCES

(1) Babich, I.; Moulijn, J. A. Science and technology of novel processes for deep desulfurization of oil refinery streams: a review★. *Fuel* **2003**, *82*, 607−631.

(2) Houda, S.; Lancelot, C.; Blanchard, P.; Poinel, L.; Lamonier, C. Oxidative Desulfurization of Heavy Oils with High Sulfur Content: A Review. *Catalysts* **2018**, *8*, 344−369.

(3) Javadli, R.; de Klerk, A. Desulfurization of Heavy Oil. *Appl. Petrochem. Res.* **2012**, *1*, 3−19.

(4) Crucianelli, M.; Bizzarri, B. M.; Saladino, R. SBA-15 Anchored Metal Containing Catalysts in the Oxidative Desulfurization Process. *Catalysts* **2019**, *9*, 984−1013.

(5) Akopyan, A. V.; Fedorov, R. A.; Andreev, B. V.; Tarakanova, A. V.; Anisimov, A. V.; Karakhanov, E. A. Oxidative Desulfurization of Hydrocarbon Feedstock. *Russ. J. Appl. Chem.* **2018**, *91*, 529−542.

(6) Akopyan, A. V.; Polikarpova, P. D.; Plotnikov, D. A.; Eseva, E. A.; Tarakanova, A. V.; Anisimov, A. V.; Karakhanov, E. A. Desulfurization of Light Distillates by Oxidation and Rectification of Gas Condensate. *Pet. Chem.* **2019**, *59*, 608−614.

(7) Zhang, J.; Wang, A.; Wang, Y.; Wang, H.; Gui, J. Heterogeneous Oxidative Desulfurization of Diesel Oil by Hydrogen Peroxide: Catalysis of an Amphipathic Hybrid Material Supported on SiO$_2$. *Chem. Eng. J.* **2014**, *245*, 65−70.

(8) Fraile, J. M.; Gil, C.; Mayoral, J. A.; Muel, B.; Roldán, L.; Vispe, E.; Calderón, S.; Puente, F. Heterogeneous Titanium Catalysts for Oxidation of Dibenzothiophene in Hydrocarbon Solutions with Hydrogen Peroxide: On the Road to Oxidative Desulfurization. *Appl. Catal., B* **2016**, *180*, 680−686.

(9) Bhadra, B. N.; Jhung, S. H. Oxidative Desulfurization and Denitrogenation of Fuels Using Metal-organic Framework-based/-derived Catalysts. *Appl. Catal., B* **2019**, *259*, 118021.

(10) Polikarpova, P.; Akopyan, A.; Shigapova, A.; Glotov, A.; Anisimov, A.; Karakhanov, E. Oxidative Desulfurization of Fuels Using Heterogeneous Catalysts Based on MCM-41. *Energy Fuels* **2018**, *32*, 10898−10903.

(11) Sikarwar, P.; Kumar, U. K. A.; Gosu, V.; Subbaramaiah, V. Catalytic Oxidative Desulfurization of DBT Using Green Catalyst (Mo/MCM-41) Derived from Coal Fly Ash. *J. Environ. Chem. Eng.* **2018**, *6*, 1736−1744.

(12) Hao, L.; Hurlock, M. J.; Li, X.; Ding, G.; Kriegsman, K. W.; Guo, X.; Zhang, Q. Efficient Oxidative Desulfurization Using a Mesoporous Zr-based MOF. *Catal. Today* **2020**, *350*, 64−70.

(13) Wang, P.; Jiang, L.; Zou, X.; Tan, H.; Zhang, P.; Li, J.; Liu, B.; Zhu, G. Confining Polyoxometalate Clusters into Porous Aromatic Framework Materials for Catalytic Desulfurization of Dibenzothiophene. *ACS Appl. Mater. Interfaces* **2020**, *12*, 25910−25919.

(14) Huang, C.; Wu, P.; Guo, Y.; Guo, Y. Facile Synthesis of Mesoporous Kaolin Catalyst Carrier and its Application in Deep Oxidative Desulfurization. *Microporous Mesoporous Mater.* **2020**, *306*, 110415.

(15) Mendiratta, S.; Ali, A. A. A. Recent Advances in Functionalized Mesoporous Silica Frameworks for Efficient Desulfurization of Fuels. *Nanomaterials* **2020**, *10*, 1116.

(16) Ali-Zade, A. G.; Buryak, A. K.; Zelikman, V. M.; Oskolok, K. V.; Tarkhanova, I. G. SILCs in Oxidative Desulfurization: Effect of Support and Heteropolyanion. *New J. Chem.* **2020**, *44*, 6402−6410.

(17) Rivoira, L.; Juárez, J.; Martínez, M. L.; Beltramone, A. Iron-modified Mesoporous Materials as Catalysts for ODS of Sulfur Compounds. *Catal. Today* **2020**, *349*, 98−105.

(18) Kulikov, L. A.; Akopyan, A. V.; Polikarpova, P. D.; Zolotukhina, A. V.; Maximov, A. L.; Anisimov, A. V.; Karakhanov, E. A. Catalysts Based on Porous Polyaromatic Frameworks for Deep Oxidative Desulfurization of Model Fuel in Biphasic Conditions. *Ind. Eng. Chem. Res.* **2019**, *58*, 20562−20572.

(19) Song, J.; Li, Y.; Cao, P.; Jing, X.; Faheem, M.; Matsuo, Y.; Zhu, Y.; Tian, Y.; Wang, X.; Zhu, G. Synergic Catalysts of Polyoxometalate@ Cationic Porous Aromatic Frameworks: Reciprocal Modulation of

Both Capture and Conversion Materials. *Adv. Mater.* **2019**, *31*, 1902444.

(20) Polikarpova, P.; Akopyan, A.; Shlenova, A.; Anisimov, A. New mesoporous catalysts with Brønsted acid sites for deep oxidative desulfurization of model fuels. *Catal. Commun.* **2020**, *146*, 106123.

(21) Yuan, Y.; Sun, F.; Ren, H.; Jing, X.; Wang, W.; Ma, H.; Zhao, H.; Zhu, G. Targeted Synthesis of a Porous Aromatic Framework with a High Adsorption Capacity for Organic Molecules. *J. Mater. Chem.* **2011**, *21*, 13498−13502.

(22) Maximov, A.; Zolotukhina, A.; Kulikov, L.; Kardasheva, Y.; Karakhanov, E. Ruthenium Catalysts Based on Mesoporous Aromatic Frameworks for the Hydrogenation of Arenes. *React. Kinet. Mech. Catal.* **2016**, *117*, 729−743.

(23) Merino, E.; Verde-Sesto, E.; Maya, E. M.; Corma, A.; Iglesias, M.; Sánchez, F. Mono-functionalization of Porous Aromatic Frameworks to Use as Compatible Heterogeneous Catalysts in One-pot Cascade Reactions. *Appl. Catal., A* **2014**, *469*, 206−212.

(24) Weber, J.; Thomas, A. Toward Stable Interfaces in Conjugated Polymers: Microporous Poly(p-phenylene) and Poly-(phenyleneethynylene) Based on a Spirobifluorene Building Block. *J. Am. Chem. Soc.* **2008**, *130*, 6334−6335.

(25) Klumpen, C.; Gödrich, S.; Papastavrou, G.; Senker, J. Water Mediated Proton Conduction in a Sulfonated Microporous Organic Polymer. *Chem. Commun.* **2017**, *53*, 7592−7595.

(26) Kulikov, L. A.; Boronoev, M. P.; Makeeva, D. A.; Nenasheva, M. V.; Egazar'yants, S. V.; Karakhanov, E. A. Hydroconversion of Naphthalene in the Presence of NiMoS/NiWS-AlCl3 Catalyst Systems Derived from Mesoporous Aromatic Frameworks. *Chem. Technol. Fuels Oils* **2018**, *53*, 879−884.

(27) Karakhanov, E.; Maximov, A.; Kardasheva, Y.; Vinnikova, M.; Kulikov, L. Hydrotreating of Light Cycle Oil over Supported on Porous Aromatic Framework Catalysts. *Catalysts* **2018**, *8*, 397.

(28) Lu, W.; Yuan, D.; Sculley, J.; Zhao, D.; Krishna, R.; Zhou, H.-C. Sulfonate-Grafted Porous Polymer Networks for Preferential CO_2 Adsorption at Low Pressure. *J. Am. Chem. Soc.* **2011**, *133*, 18126−18129.

(29) Goesten, M. G.; Szécsényi, À.; de Lange, M. F.; Bavykina, A. V.; Gupta, K. B. S. S.; Kapteijn, F.; Gascon, J. Sulfonated Porous Aromatic Frameworks as Solid Acid Catalysts. *ChemCatChem* **2016**, *8*, 961−967.

(30) Zhang, W.; Cheng, Y.; Guo, C.; Xie, C.; Xiang, Z. Cobalt Incorporated Porous Aromatic Framework for CO_2/CH_4 Separation. *Ind. Eng. Chem. Res.* **2018**, *57*, 10985−10991.

(31) Goesten, M. G.; Juan-Alcañiz, J.; Ramos-Fernandez, E. V.; Sai Sankar Gupta, K. B.; Stavitski, E.; van Bekkum, H.; Gascon, J.; Kapteijn, F. Sulfation of metal-organic frameworks: Opportunities for acid catalysis and proton conductivity. *J. Catal.* **2011**, *281*, 177−187.

(32) Juan-Alcañiz, J.; Gielisse, R.; Lago, A. B.; Ramos-Fernandez, E. V.; Serra-Crespo, P.; Devic, T.; Guillou, N.; Serre, C.; Kapteijn, F.; Gascon, J. Towards Acid MOFs - Catalytic Performance of Sulfonic Acid Functionalized Architectures. *Catal. Sci. Technol.* **2013**, *3*, 2311−2318.

(33) Zhu, W.; Li, H.; Gu, Q.; Wu, P.; Zhu, G.; Yan, Y.; Chen, G. Kinetics and Mechanism for Oxidative Desulfurization of Fuels Catalyzed by Peroxo-molybdenum Amino Acid Complexes in Water-immiscible Ionic Liquids. *J. Mol. Catal. A: Chem.* **2011**, *336*, 16−22.

(34) Kulikov, L. A.; Maksimov, A. L.; Karakhanov, E. A. Diesel Fraction Hydrotreating in the Presence of Nickel-Tungsten Sulfide Catalyst Particles In Situ Synthesized in Pores of Aromatic Polymers. *Pet. Chem.* **2019**, *59*, 66−71.

(35) Karakhanov, E.; Maximov, A.; Kulikov, L.; Makeeva, D.; Kalinina, M.; Kardasheva, Y.; Glotov, A. Evaluation of Sulfide Catalysts Performance in Hydrotreating of Oil Fractions Using Comprehensive Gas Chromatography Time-of-flight Mass Spectrometry. *Pure Appl. Chem.* **2020**, *92*, 941−948.